NATIONAL RADIO ASTRONOMY OBSERVATORY
Green Bank, West Virginia

Electronics Division Internal Report No. 119

A LASER DISTANCE MEASURING INSTRUMENT

John M. Payne

JUNE 1972

NUMBER OF COPIES: 150

A LASER DISTANCE MEASURING INSTRUMENT

John M. Payne

CONTENTS

LIST OF FIGURES

TABLES

A LASER DISTANCE MEASURING INSTRUMENT

1.0 Summary

This report describes a prototype distance measuring instrument that may be used to survey the surface of a radio telescope in a fast and accurate manner. The principle used is simply to measure the transit time of a beam of light out and back over the path to be measured.

The instrument will permit a survey using a triangulation method by making accurate range measurements over two paths to small reflectors on the surface of the telescope.

The instrument in its present form will measure ranges up to 60 meters with an RMS (1σ) accuracy of better than $\pm$ 0.1 mm and in a measurement time of 2.5 seconds.

2.0 Introduction

The birth of this instrument has been precipitated by the completion of the design of the 65 meter telescope. A critical part of the construction of the telescope will be the setting and subsequent checking of the surface panels, a task usually accomplished by measurements using a tape and theodolite. The design of the telescope requires setting about 3,000 points on the surface to an accuracy of $\pm$ 0.1 mm RMS in a few hours, an almost impossible task using conventional methods.

Although the instrument described in this report was developed primarily to prove the feasibility of a performance adequate for the setting of the 65 meter telescope, it may well prove useful in surveying existing instruments. Interest has been expressed in using the instrument for setting the new surface at Arecibo and the instrument, when repackaged, would be ideal for this application. No problems are anticipated by operation at a range of 150 meters.

The instrument uses a simple principle that has been used for many years in surveying instruments. Commercial instruments using this principle are available but the best have an accuracy of only $\pm$ 1 mm which is not adequate for our needs.

3.0 Principle of Operation

A high-intensity light beam (in our case a helium neon laser beam) is amplitude modulated, transmitted over the path to be measured, and reflected back to the instrument. The phase of the returned beam is measured with respect to a reference, the phase shift being proportional to the total distance the transmitted light beam has travelled.

This principle is illustrated in Figure 1 in which the light beam is modulated at a frequency f_m, the one-way distance to be measured is d, and the phase of the returned signal is ϕ_s.

The returned light beam will be shifted in phase by $\frac{2d}{\lambda}$ where λ is the wavelength of the modulating frequency. If $\lambda < 2d$, then the phase will be shifted through more than one cycle and ambiguities in distance reading will arise.

The instrument we have developed uses a modulating frequency of 550 MHz, so range ambiguities will occur about every 27 cm. This means, of course, that the distance to be measured has to be known in advance to better than this value. A dual-frequency system is often used to resolve such ambiguities, and the present instrument could be modified to work in this way. However, it seems unnecessary for measuring radio telescopes.

Referring to Figure 1, the phase detector output will be proportional to

$$\phi_r - \phi_s$$

where ϕ_r is the reference phase and ϕ_s is the phase of the returned signal.

$$\phi_s = \frac{2d - n\lambda}{\lambda} \times 360 \text{ degrees}$$

where $(2d - n\lambda) < \lambda$ and n is an integer.

For a distance determination of 0.1 mm accuracy using a λ of 55 cm, we require a phase measuring accuracy and phase stability within the instrument of 0.13°.

The high accuracy of the instrument stems directly from the high modulation frequency used. The highest frequency used in a commercial instrument is 75 MHz for which the manufacturer claims an accuracy of ± 1 mm.

The velocity of light through air varies with air temperature, pressure, and relative humidity. At a range of 60 m we need to know air temperature to about 1.5 °C and air pressure to about 4 mm of mercury to achieve the 0.1 mm accuracy. The effects of relative humidity over such a distance can be neglected.

4.0 Existing Instruments

There are many ways of implementing the simple principle illustrated in Figure 1 and Table 1 gives a summary of various instruments using this general principle. An instrument coming very close in performance to our requirements is the Mekometer III that was developed at the National Physical Laboratory in the U.K. This instrument is not at present commercially available.

The Mekometer uses an ingeneous phase measuring technique that nulls the phase of the received light beam by mechanically changing the path length of the received signal a calibrated amount. By slightly shifting the transmitted signal in frequency and re-nulling several times the distance may be obtained. This method has the advantage of eliminating any errors inherent in the measurement of phase electronically but is not suitable for our application due to the fairly long period required for a measurement.

Some of the instruments listed in Table 1 overcome any potential instability in the phase measuring circuits by switching between an internal optical reference path and the signal path in a manner similar to a load-switched radiometer.

Our previous experience with mixers and phase measuring techniques suggested that mixing down the 550 MHz signal and reference waveforms to a low frequency and comparing the phases directly should yield a measurement accuracy of 0.1° in phase.

Before building the instrument we tested various R. F. components (hybrids, filters, amplifiers and mixers) and reached the conclusion that provided the components were stable in temperature to better than ± 1 °C the phase detection to 0.1° was certainly feasible.

Before building the prototype instrument we decided that the instrument should have the following specifications:

Accuracy better than ± 0.1 mm RMS
on a single reading.
Range: 1 m - 60 m.
Measurement time less than 5 secs.
Digital display automatically updated.
Reflector size 1" diameter or less.

5.0 Description of Instrument

5.1 General

A photograph of the instrument and its display unit is shown in Figure 2. More detailed views of the instrument are shown in Figure 3. Cigarette smoke was blown in to make the laser beam visible. No effort was taken to make the instrument small; like most prototypes, it just grew. For the final tests of the instrument, it was housed in a temperature controlled box, the light beam passing through a quartz window. A block diagram of the instrument is shown in Figure 4.

5.2 Choice of Frequencies

There are three main frequencies within the instrument:

1) The modulating frequency.
2) The IF frequency.
3) The digital circuitry clock frequency.

To achieve the stability required it seemed essential that these frequencies be derived from a common, stable, crystal oscillator.

Corrections for variation in the speed of light due to changes in atmospheric conditions may also be applied directly to the instrument by pulling the frequency of this master oscillator. The frequencies were chosen as follows:

Master Oscillator .... $f_o = 60.97463$ MHz

Modulating Frequency .... $f_m = 9f_o = 548.7717$ MHz

IF Frequency .... $f_{IF} = \frac{f_o}{2^{14}} = 3.72160$ kHz

Clock Frequency .... $\frac{f_o}{3} = 20.32487$ MHz

With these frequencies and the group* velocity of light at 0 °C and 760 mm of mercury the digital phase meter will have a sensitivity of 20 counts per millimeter of distance per cycle of IF signal, and the digital display may be arranged to read directly in cm, the least significant digit being 0.001 cm.

---

* The group velocity is correctly used since it is the velocity of the modulation envelope which is required.

5.3 Optics

The optics of the instrument were kept very simple and no effort was directed towards compactness. A more engineered version of the instrument could be made much smaller by using a shorter focal length receiving mirror.

The light source we used was a Hughes Helium Neon Laser Model 3076H. This laser has a power output of 3 mW, a beam divergence of 0.8 milliradian, and is linearily polarized to better than 1000:1.

The optical path is made clear from Figure 4. The polarized laser beam first passes through a cavity that is tuned to the modulating frequency. In the high electric field region of the cavity is a crystal of potassium dihydrogen phosphate (KDP) through which the laser beam passes. When an electric field is applied to this crystal the plane of polarization of the laser beam is rotated. On emerging from the cavity the beam passes through a polarizing prism that converts the polarization angle modulation to amplitude modulation.

Two mirrors then direct the beam to the distant target which is a retroreflector. This has the property of reflecting the light beam back along its path with a high degree of precision over a wide range of angles of the incident light.

The returned light beam has a diameter of about 3 inches at the receiving mirror at a range of 60 m. This light is then focused, via a mirror, onto the receiving photo diode.

For linear operation of the instrument it is essential that no modulated laser light, other than the directly reflected beam, find its way into the receiving diode. It is also important that there are no multiple reflections between the diode and the distant reflector. This is explained more fully later.

5.4 Electronics

5.41 Signal Flow

The master oscillator drives a x3 transistor multiplier and power amplifier that provides 500 mW at 182.92389 MHz to the x3 transistor multiplier built into the top part of the cavity. This multiplier provides 1 watt at 548.7717 MHz to the modulating crystal.

The master oscillator is divided by a 14-bit counter to produce a 3.72160 kHz signal which is added to the modulating frequency to produce the local oscillator frequency via the LO circuits.

The received light signal is first detected and amplified in the avalanche photodiode which is matched to 50 ohms at 550 MHz. The 550 MHz signal is now filtered, amplified and mixed to produce an IF signal at 3.72160 kHz. This signal is squared using a Schmitt trigger and the leading edge is used to start the clock pulses at 20.324878 MHz into the integrating digital phase detector. The clock pulses are stopped by the leading edge of the reference signal, the accumulated clock pulses being a measure of the phase difference between the two waveforms.

The digital circuitry permits the averaging of 100, 1000, or 10,000 IF signal periods, the number of periods being selectable by a switch.

As previously mentioned, the frequencies have been chosen to give a scale factor of 20 clock pulses per millimeter for one IF cycle. At the end of an integration period, which then includes the sum of many IF cycles, the accumulated count is displayed on a 5-digit L.E.D. display in centimeters, the least significant digit being 0.001 cm.

5.42 Modulator

The modulator assembly is shown in Figure 5. The KDP crystal was purchased from Isomet Corporation sealed in a plastic case with optical windows coated for 6328 Å. The crystal needs a DC bias of about 500 volts to ensure operation in the linear region and an RF voltage of 200 V p.p. to give a modulation depth of around 10 percent. We decided the best solution to the problem of driving the modulator would be to incorporate it in a cavity.

We found that the case the crystal was encapsulated in was rather lossy and reduced the Q of the cavity, resulting in an RF drive level of about 1 watt.

The cavity was fine tuned by an adjustable vane giving variable capacitance between the center conductor and the floor of the cavity.

The final x3 multiplier was situated in the top of the cavity and was coupled into the cavity via a loop to the center conductor. This loop was arranged to give an input impedance of 50 ohms to simplify testing of the multiplier and cavity.

Another loop in the top of the cavity served to couple out about 10 mW of power at 550 MHz for the local oscillator circuits.

A crucial part of the design of the instrument is the prevention of any of the RF modulating signal leaking into the received signal path. This isolation was achieved by putting the RF power circuits in the top of the cavity, having a good fitting lid on the cavity and also by double shielding the receiver.

5.43 Multiplier Chain

The RF multiplier chain is shown in Figure 6 and is conventional in design. We used an RCA "overlay" transistor for the final multiplier and found that the voltage variable collector to base capacitance permitted very efficient multiplication.

5.44 Digital Divide Circuits

The digital divide circuits are shown in Figure 7. The master oscillator signal passes through a buffer amplifier and logic gates and is then divided by three to produce the clock frequency for the phase detector and display circuitry and also drives a 14-bit counter to give the 3.72160 kHz signal to the local oscillator circuits.

5.45 Local Oscillator Circuits

The local oscillator circuits are shown in Figure 8. A voltage-controlled crystal oscillator running at approximately 60.947 MHz is multiplied by nine in a transistor multiplier and filtered through a narrow band cavity filter. The output from the multiplier is then split with a hybrid, one output providing the system local oscillator, the other output feeding a mixer via a circulator and a 20 dB pad. The LO port of this mixer is fed with +7 dBm at the modulating frequency from the cavity. The IF output of this mixer is then amplified and mixed with the 3.72160 kHz signal from the digital divide circuits. The output of this mixer is amplified and passed through a low-pass filter and applied to the voltage-controlled crystal oscillator. With this phase-locked loop in a "locked" condition, the LO output will always be exactly 3.72160 kHz away from the modulating frequency.

5.46 Receiving Circuits

The receiving circuits are shown in Figure 9. The photodiode, bandpass filter, RF amplifier, mixer, and IF amplifier are all mounted inside a double-shielded box attached to the side of the receiving telescope. The diode and matching circuits are contained in a separate shielded box. Care was taken to screen and decouple all supply leads into the receiver box.

The Schmitt trigger was used rather than a straight limiter to avoid false triggering of the digital readout circuits through noise on the zero crossing of the IF signal. The main reason for the filter in the signal line was to reject a strong signal at 500 MHz that results from a longitudinal mode of oscillation in the laser. This signal was rejected because of the possibility of intermodulation products in the mixer.

5.47 Integrating Phase Detector

The 3.7 kHz start (reference) and stop (signal) square waves enter the phase detector through D-type flip-flops and both are delayed by one clock pulse. (The clock is about 20 MHz.)

The output of gate A, pin 14, will be a burst of clock pulses at the 3.7 kHz IF, the number of pulses being proportional to the phase difference between the signal and reference IF waveforms. The clock pulses are then gated into the display counter (F, etc.) via the counters B, C, D and the flip-flop E.

The circuitry permits the averaging of phase differences for 100, 1000, or 10,000 cycles of the IF. For example, for averaging 100 cycles of the intermediate frequency, the counter B divides the clock pulses representing phase shift by 100. After 100 IF cycles, determined by the "enable" counters, the clock pulses accumulated in the display counter are gated into the display.

Operation is similar in the averaging of 1000, or 10,000, cycles and the display counter always counts up in increments of 0.001 cm.

6.0 Theoretical Performance of Instrument

6.1 Signal-to-Noise Ratio

The transmitted light beam is attenuated somewhat by the various optical components and the actual transmitted power is about 1 mW. With a 1" target retroreflector, a beam divergence of 0.8 milliradian and a 3" diameter receiving mirror, the power at the photodiode is about 0.2 mW. This results in such a high signal-to-noise ratio that negligible phase noise results.

There are other sources of noise, however, that can only be evaluated by measurement. The other noise contributions come from A. M. noise on the laser and intensity fluctuations of the returned light due to atmospheric irregularities and instabilities. The noise contribution from the laser was measured in the lab and was found to be negligible.

6.2 Signal Leakage

Any small signal at the modulating frequency finding its way into the receiver will add to the desired signal and produce phase errors which will in turn produce cyclic errors in the measured distance with a spatial periodicity of half a wavelength (27.3 cm). The isolation required between the inside of the cavity and the input to the receiver is about 140 dB to keep phase errors as low as 0.01°.

6.3 Oscillator Stability

The required stability for the crystal oscillator for an accuracy of ± 0.1 mm in 60 m is 1 part in 6×10^5 which is easy to achieve with a crystal oscillator in a temperature enclosed environment.

6.4 Atmospheric Effects

The atmosphere affects the instrument in several different ways.

1) Short term effects giving angular fluctuations in the beam. When a beam of light is projected over a path close to the ground it is subject to turbulence that can be severe at times. During our tests we found angular deviations as much as 0.2 milliradian peak to peak. This caused the returned signal to vary greatly in strength and at times drop to zero. As would be expected, under these conditions the accuracy of the instrument was decreased. This condition occurred only rarely, generally when the

weather was sunny and calm. Our experiments with the optical reference platform on the 140-foot telescope suggest that these effects are greatly reduced a few feet above the surface of the ground.

2) Short term effects giving changes in refractive index. The effects mentioned above are due to "blobs" of air at slightly different temperatures through the beam. These blobs will have the effect of continually changing the effective refractive index of the light path. No calculations have been made on this effect: experiments show it to be very small.

3) Variation in refractive index with atmospheric conditions. The group refractive index of air is given by the equation

$$n_g = 1 + \frac{(n_{go} - 1)}{1 + \frac{t}{273.15}} \times \frac{p}{760} - \frac{5.5\, e \times 10^{-8}}{1 + \frac{t}{273.15}}$$

where n_{go} = group refractive index of air at 0 °C, 760 mm Hg, water vapor pressure = 0, 0.3% CO_2 = 1.000300 for the helium neon laser frequency.

p = pressure in mm Hg.

e = partial pressure of water vapor in mm Hg.

t = temperature in °C.

From this equation we obtain the following:

a) $\frac{dn_g}{dp}$ for constant t

t °C	$\frac{dn_g}{dp}$ per mm Hg
-10	4.1005×10^{-7}
0	3.9504×10^{-7}
10	3.8109×10^{-7}
20	3.6809×10^{-7}
30	3.5595×10^{-7}

b) $\frac{dn_g}{dt}$ at constant pressure

p mm Hg	t °C	$\frac{dn_g}{dt}$ per °C
760	-10	-11.8426×10^{-7}
760	0	-10.9914×10^{-7}
760	10	-10.2288×10^{-7}
760	20	-9.5428×10^{-7}
760	30	-8.9237×10^{-7}

c) $\frac{dn_g}{de} = 0.55 \times 10^{-7}$ per mm Hg and changes negligibly with temperature and pressure. The effects of varying e from a dry to a saturated atmosphere change the range of 60 meters by less than 0.1 mm.

To give a 0.1 mm accuracy in a 60 meter range, we need to know:

Temperature to approximately 1.5 °C

Pressure to approximately 4 mm Hg

We anticipate that in use on a telescope a reference target would be used to calibrate out instrumental and atmospheric instabilities so even the simple corrections outlined above may be unnecessary.

7.0 Tests with Instrument

The first tests were performed over short path lengths in the laboratory. The target was moved on a micrometer stage and the calibration of the instrument checked and found to be correct.

As usual with this kind of project, there were many different configurations tried and discarded. Perhaps the most significant of these was the way in which the reference waveform was derived. Initially we felt that the "safest" way of deriving the reference waveform was to split the outgoing light and use a second photodiode and mixer to obtain the IF signal. After careful testing we found this to be unnecessary and used the more direct approach shown in the block diagram.

The instrument in its early days had the signal photodiode, mixer and IF amplifier in separate boxes. We found this to be far from ideal so far as leakage was concerned: much better performance was obtained when all these components were packaged together in one doubly-shielded box.

The outdoor tests were performed over a 60 m range (total path = 120 meters) with the instrument in the Reber dish building and the reflector on a micrometer bench in a small hut. The photographs in Figures 11, 12 and 13 show the arrangement.

The instrument stability over the 60 m range was first checked and gave the results shown in Figure 14, curve A.

The target was then moved in increments of one inch over a total of 32 inches and the digital readout recorded for each inch. A typical result is shown in Table 2. For a 360° phase change the display will read 27.307 cm, so this number is added to the displayed number at each crossover.

An analysis of the results given in Table 2 gives a slope of 2.540180 cm/in and a standard deviation on a single measurement of 0.00757 cm. The errors for each inch are plotted in curve B, Figure 14, and can be seen to be not noise-like but follow a cyclic pattern. This cyclic error is made clearer in the results of Figure 14, curve C. We subtracted out the repetitive features of curve C with the results shown in curve E which yielded a standard deviation of ± 0.043 mm on a single reading. The cyclic errors are, we think, due to leakage of the modulating signal into the receiver.

These results suggest that the accuracy of an engineered instrument may well be better than 0.05 mm.

8.0 Telescope Installation

A possible way of installing the instrument on a telescope is shown in Figure 16. B is regarded as a fixed point near the vertex of the dish and C is a fixed point near the focus. The distance from the instrument reference plane to the reflector at D via the mirror at B is first measured. Mirror B is then tilted out of the beam and the distance from the instrument to D via mirror C is measured.

Provided the angle CDB is less than 45° a single corner cube may be used: for angles of incidence separated by more than 45° the reflector assembly would have to use two corner cubes.

One possible way of steering the mirrors would be use a coarse positioning system (several arc minutes) to direct the beam onto the corner cube and then servo control the mirror via a quadrant detector in the returned beam. With the mirror servo controlled in this manner the time taken to go from target to target would be very short, certainly less than one second.

A system such as this would be necessary when attempting to survey the 140-foot at different telescope positions as we know the focal point moves by about 1/2". With an open loop system this movement would result in misdirecting the beam onto the reflector.

A good first installation on the 140-foot would be to incorporate the mirror at B with the instrument so making a complete unit and just measure the path ABD for about ten reflectors. The reflectors could be made to use existing target holes. This installation would require virtually no telescope time and the structure at the vertex is ideal for mounting the instrument. If these first tests were successful it would be a simple matter to add another mirror at the focal point.

9.0 Future Development

If we continue work on this instrument the next step will almost certainly be telescope installation of a more engineered version of the present instrument.

There is another development that may be worth pursuing and that is using the surface of the dish as the reflector. Argon lasers (or CO_2) are now readily available with output powers of several watts. The output of such a laser, when focused to a spot on the surface of the dish, would provide adequate power to the receiver just by scattering.

It will be realized that this report deals mainly with observation to the distant end of the 60 m baseline. The location of the zero-point of the instrument has not been determined. However, the stability observations (paragraph 7) determine that both these points remain stable to better than ± 0.1 mm. In practice, short range measurements would be made to reference targets close to the instrument as well as long range measurements to targets of interest.

In conclusion, we may say the instrument in its present form satisfies the requirements of the 65 meter telescope (± 0.1 mm RMS) and when rebuilt in a form suitable for use on a telescope there are indications that this accuracy may be doubled.

10.0 Acknowledgments

C. Pace in Charlottesville who designed and built the digital circuits, Dr. J. W. Findlay who worked on the testing of the instrument and analyzed the results, and Steve Mayor and Ralph Becker in Green Bank who built the instrument.

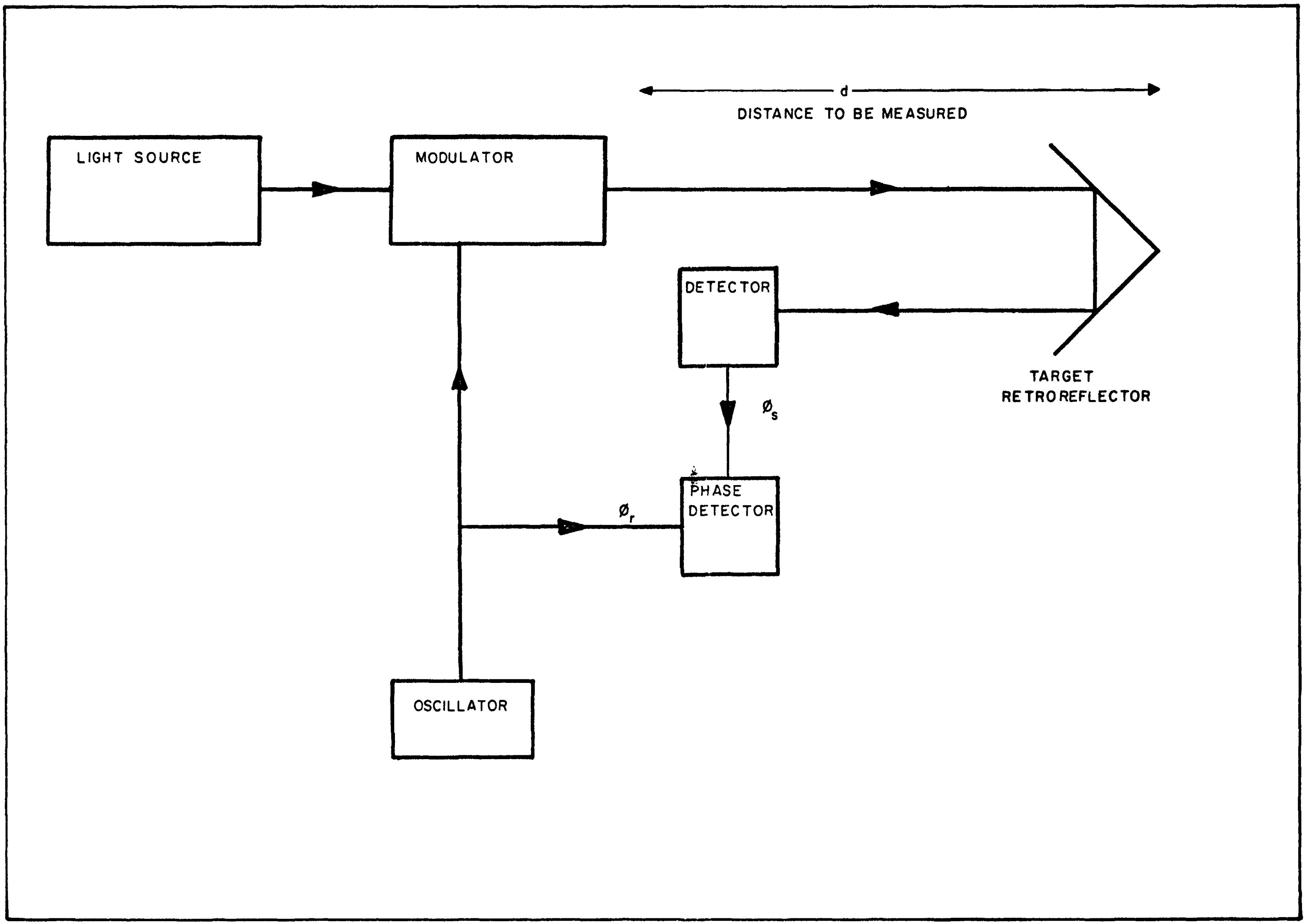

Figure 1 — Simplified Block Diagram

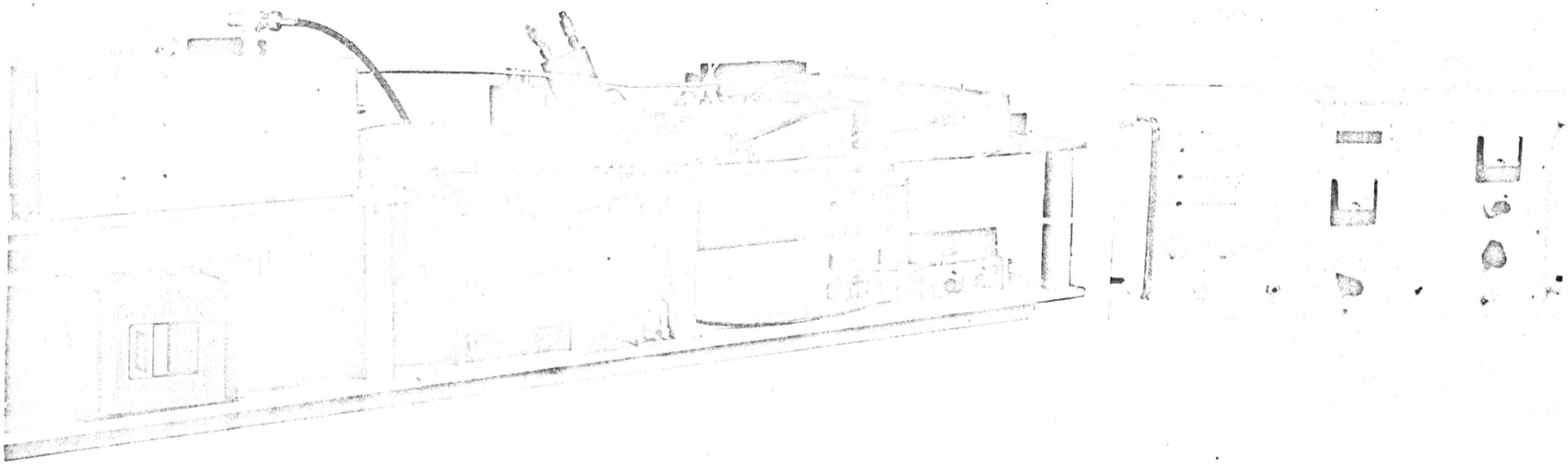

Figure 2 — Photograph of Instrument and Display Unit

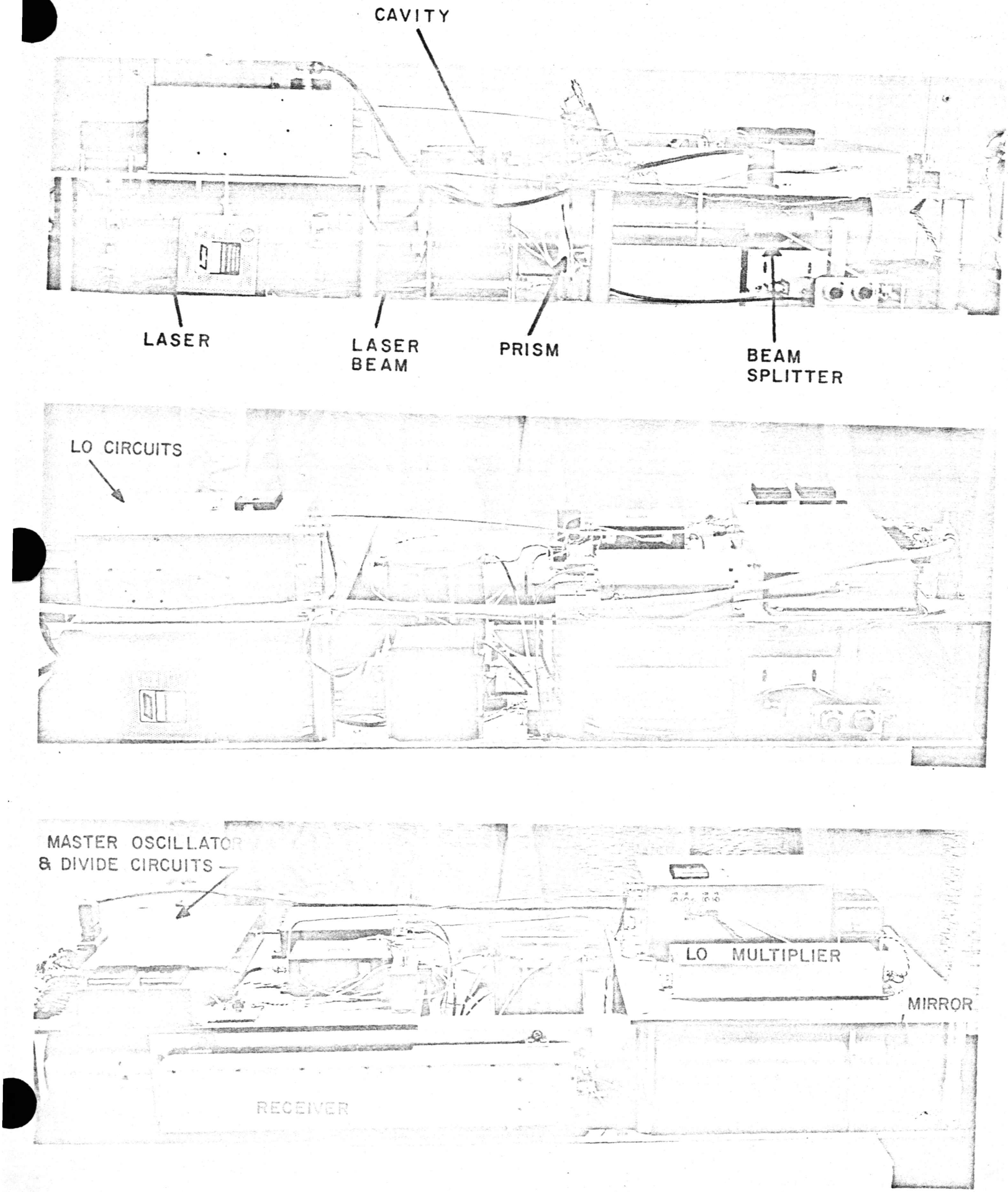

Figure 3 — Photograph of Instrument

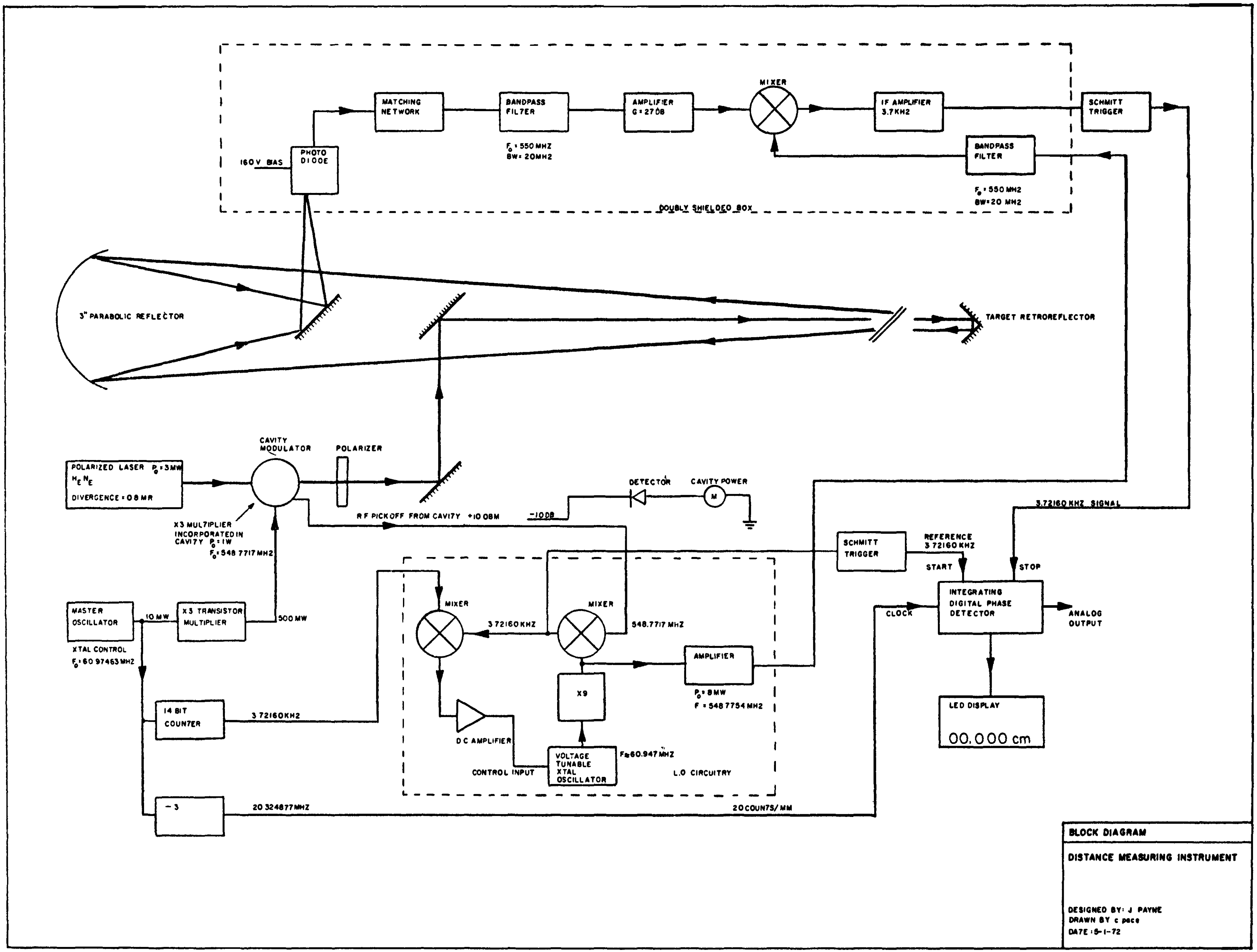

Figure 4 — Block Diagram

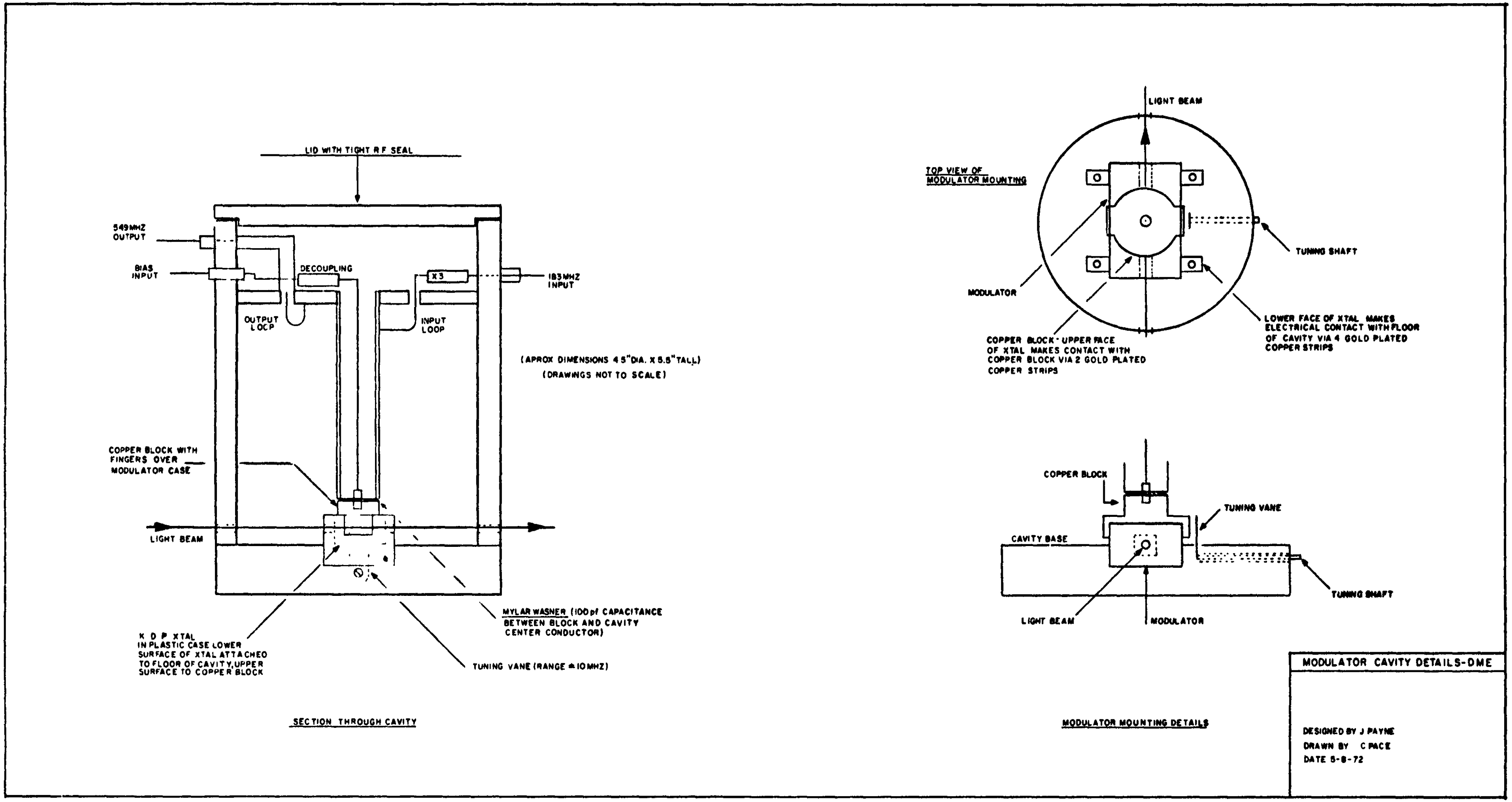

Figure 5 — Modulating Cavity

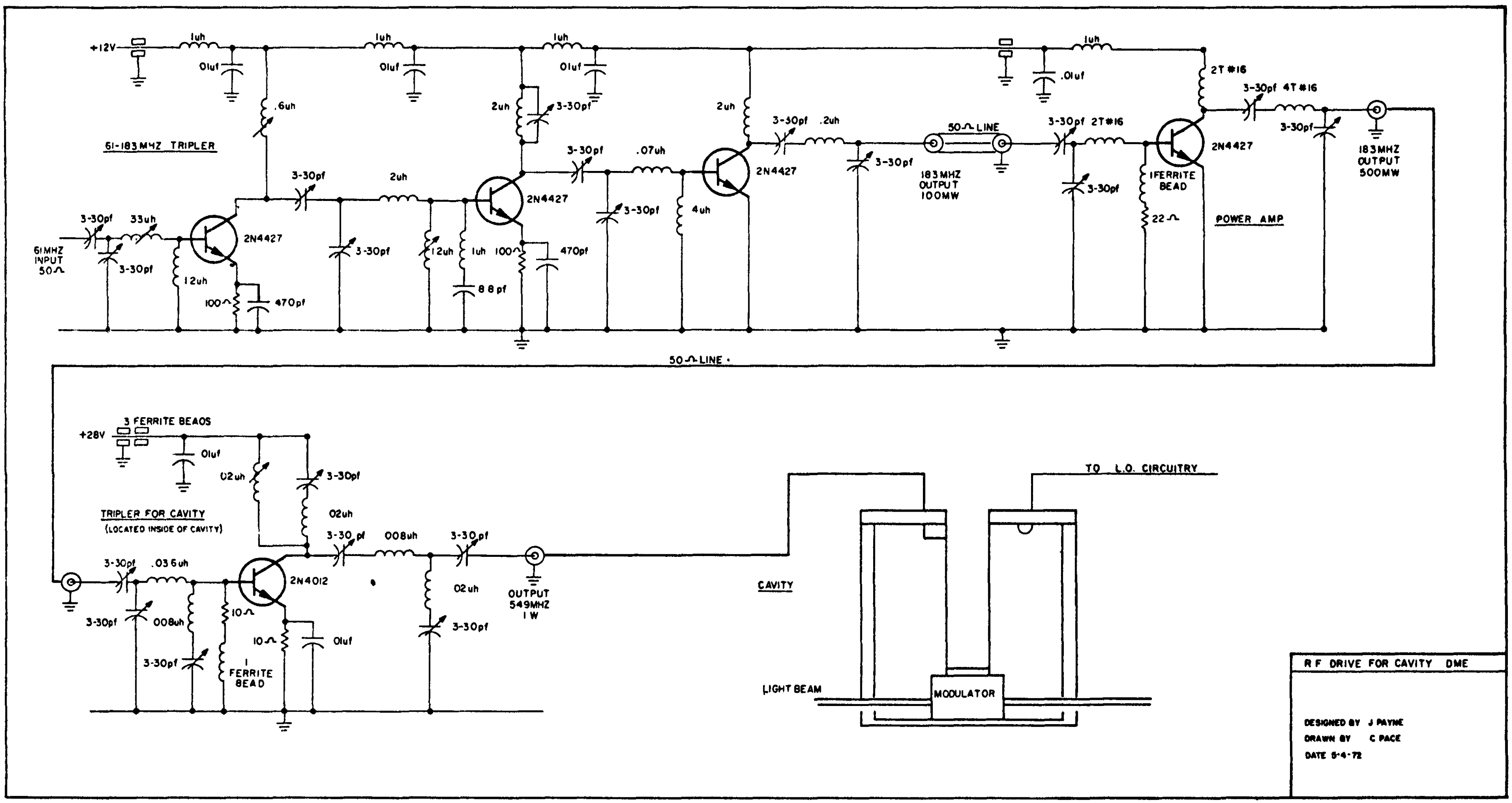

Figure 6 — RF Drive for Cavity

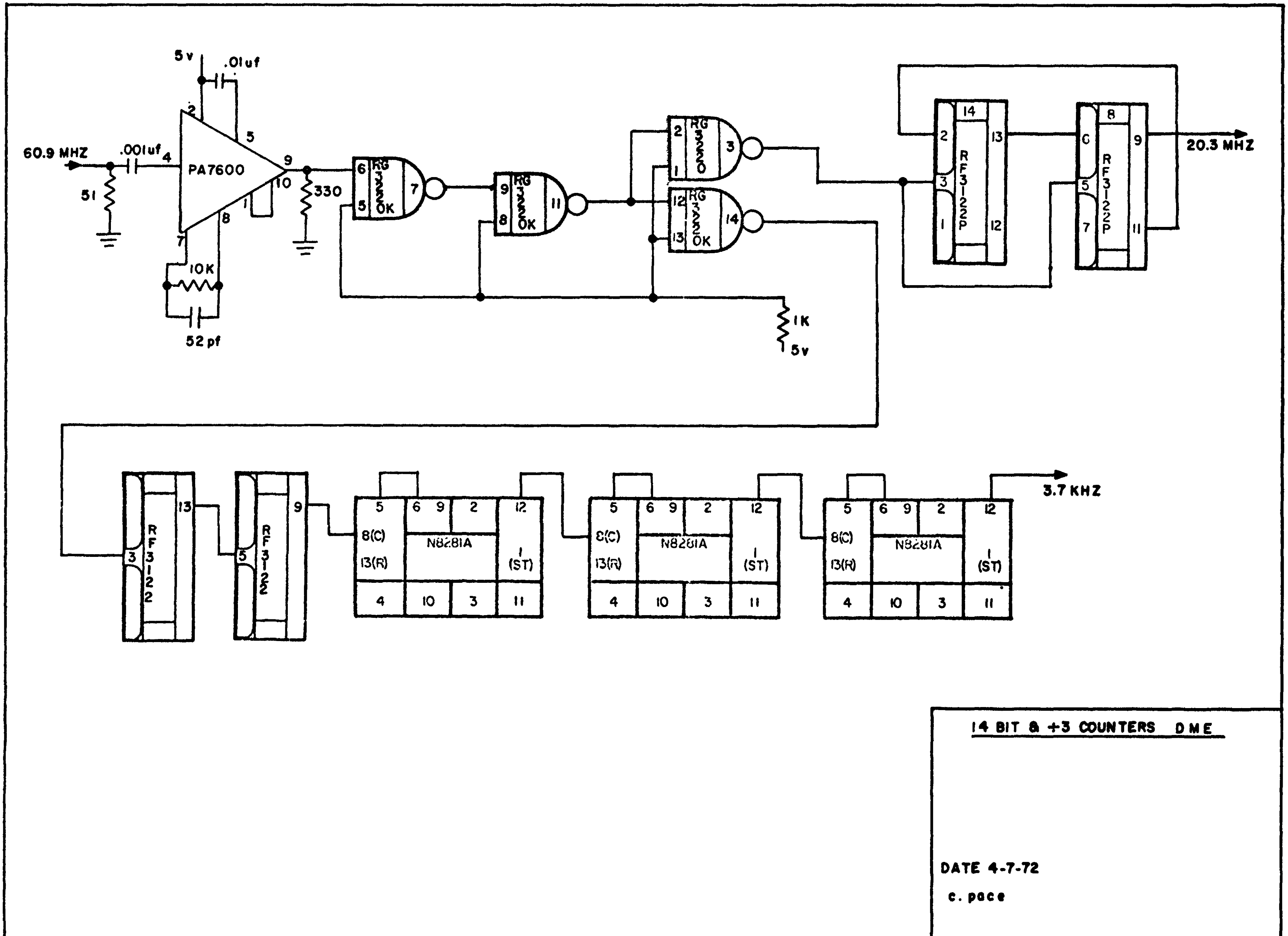

Figure 7 — Digital Divide Circuits

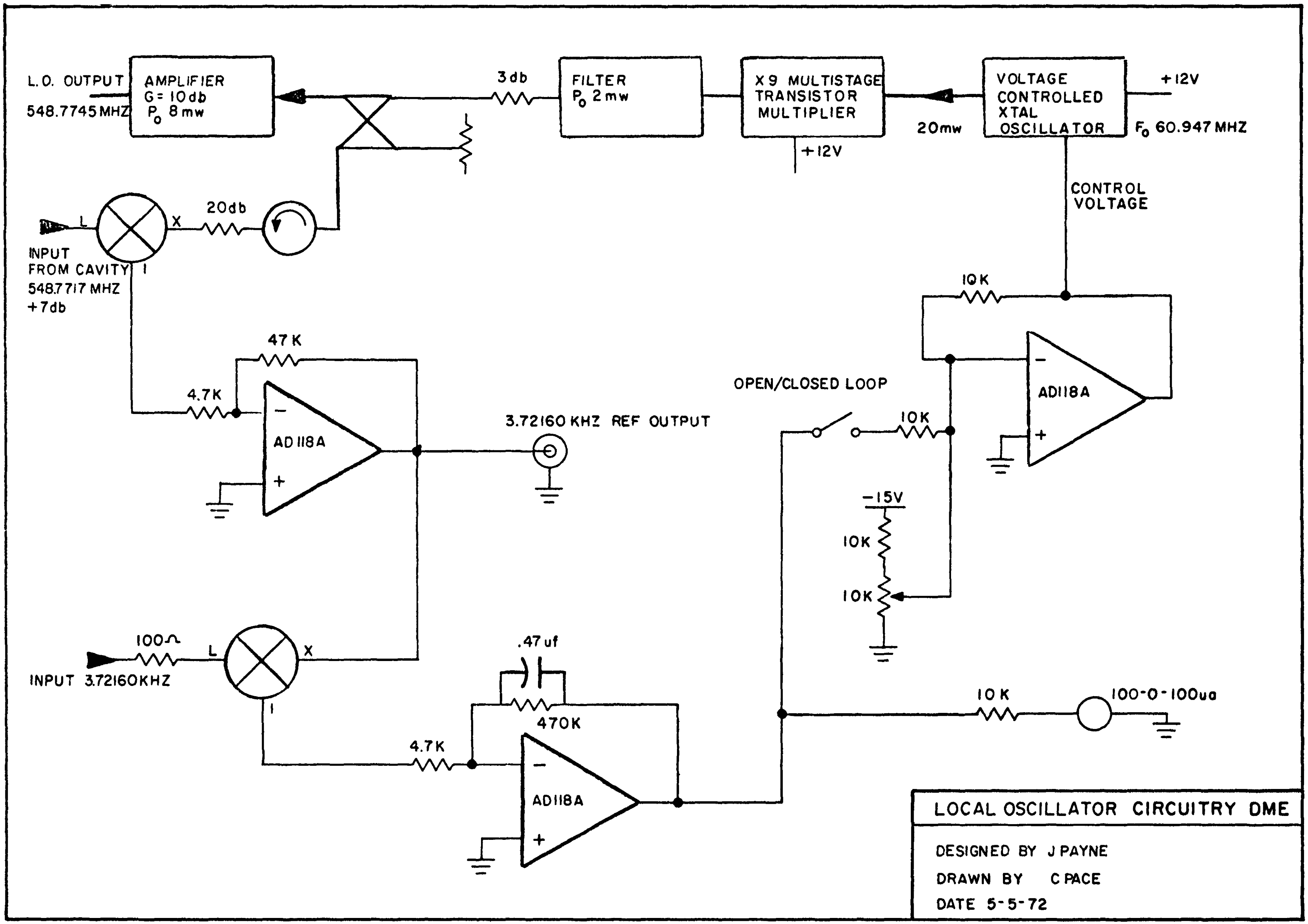

Figure 8 — Local Oscillator Circuits

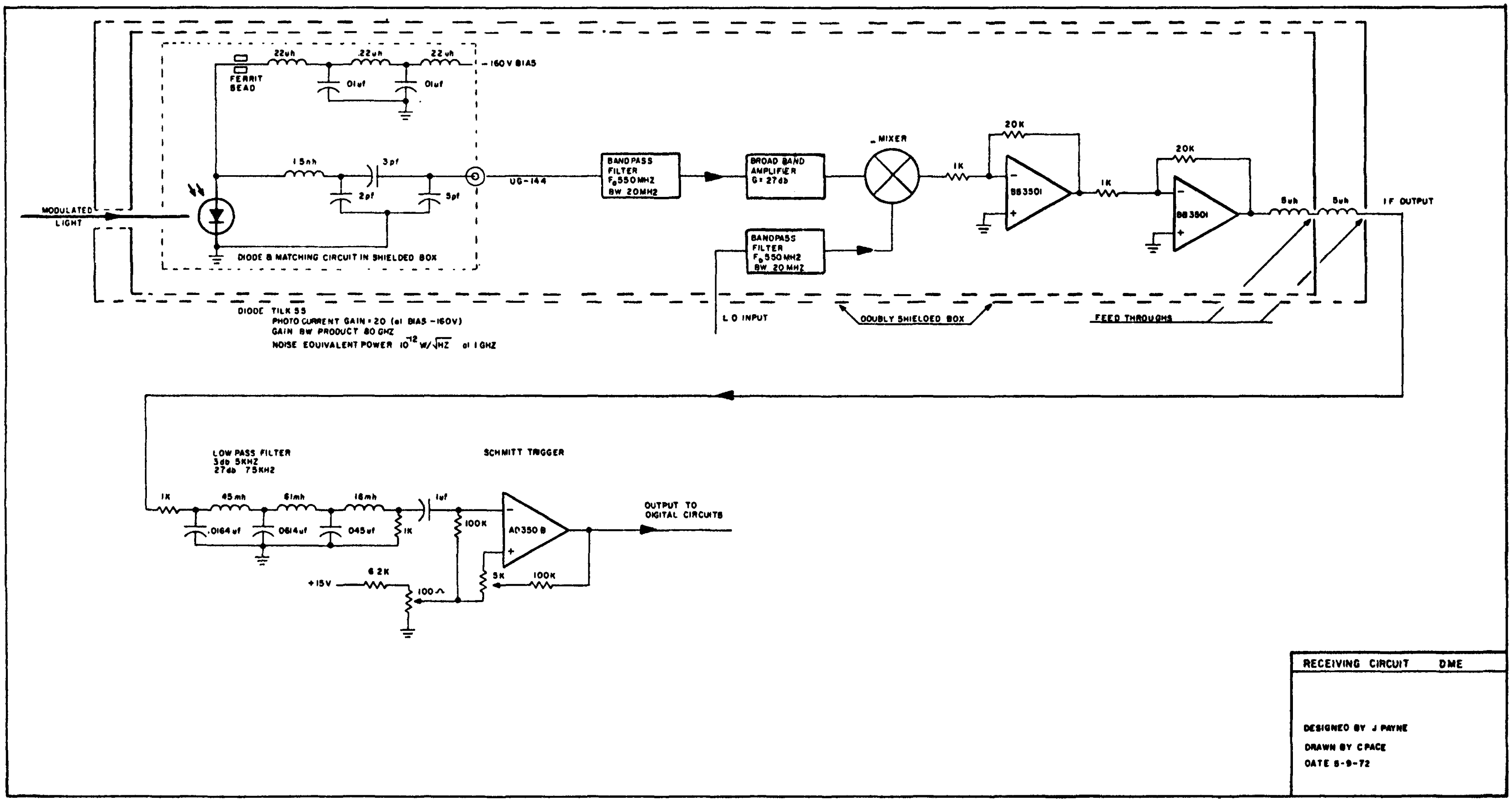

Figure 9 — Receiving Circuits

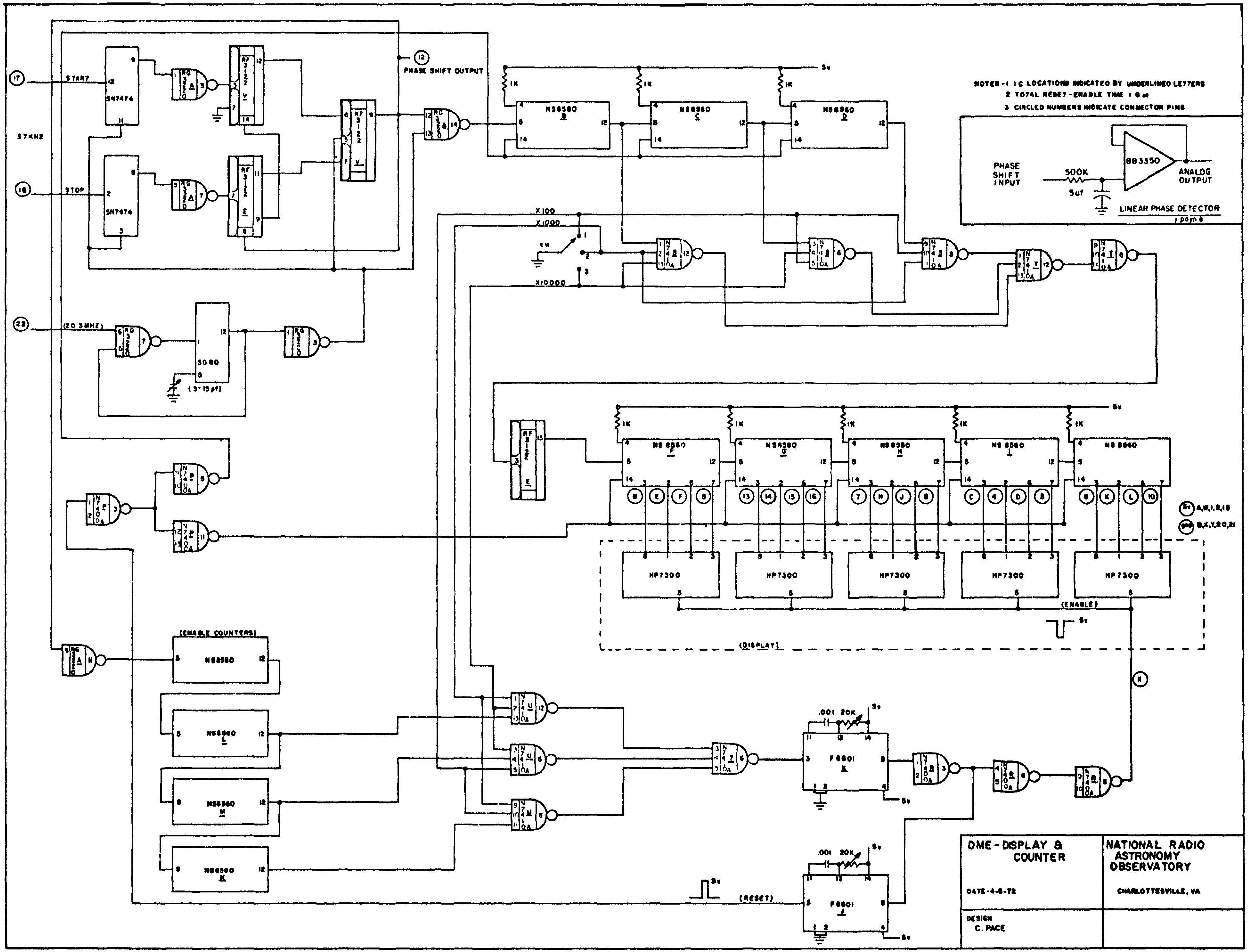

Figure 10 — Integrating Phase Detector

Figure 11 — Photograph of Test Range

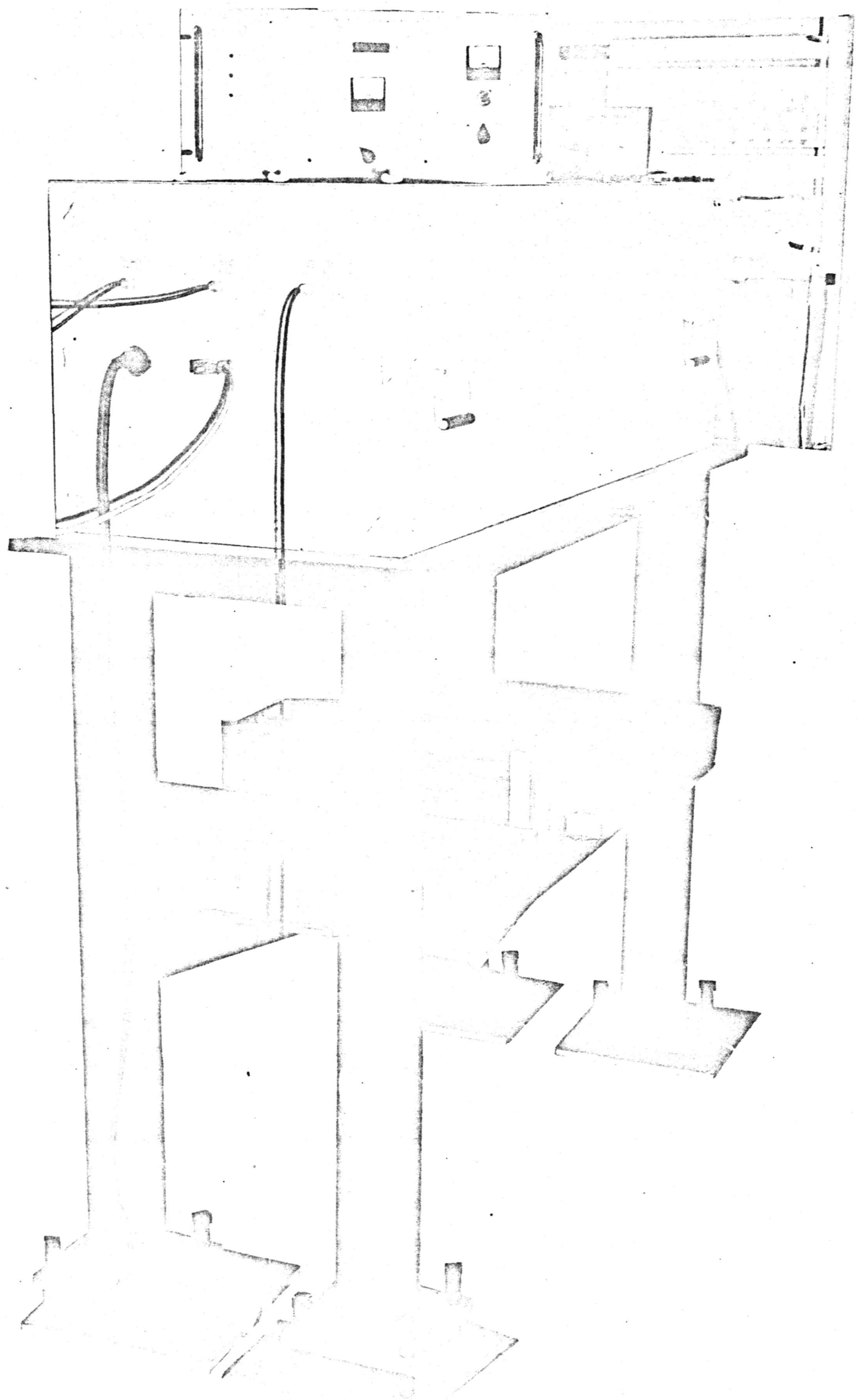

Figure 12 — Photograph of Instrument in Reber Dish Building

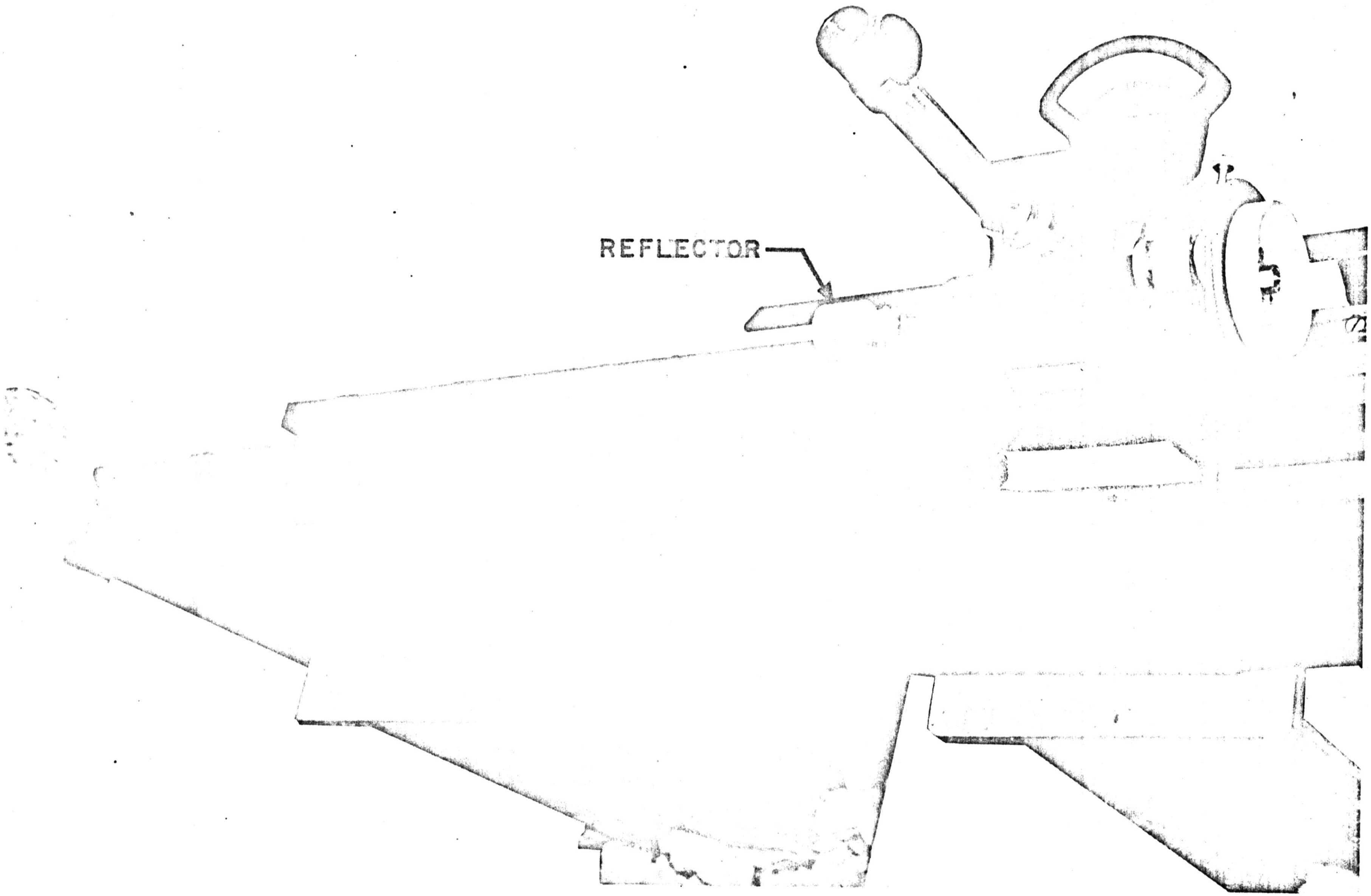

Figure 13 — Photograph of Micrometer Bench

RESULTS

A.

INSTRUMENT STABILITY — OVER RANGE OF 60 METERS

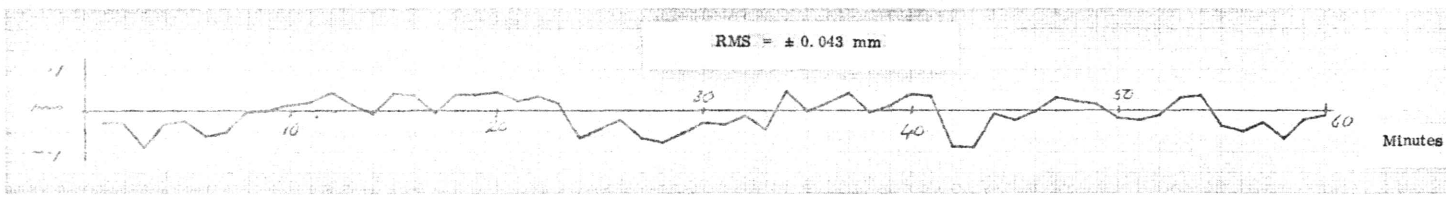

B. TYPICAL RESULT

DISTANCE MEASUREMENT — OVER RANGE OF 60 METERS

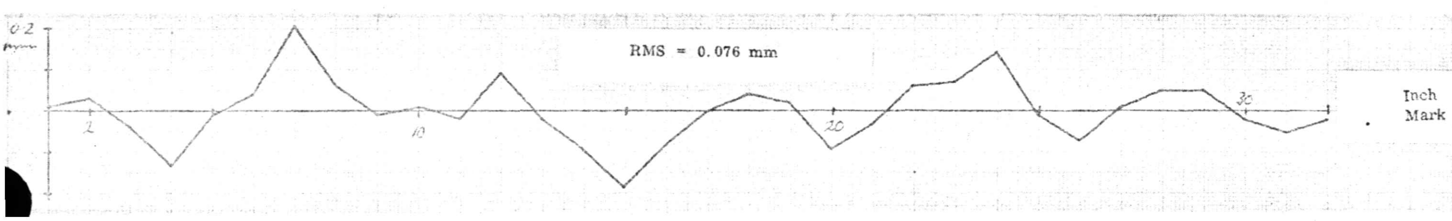

C. HIGH LEAKAGE RESULT

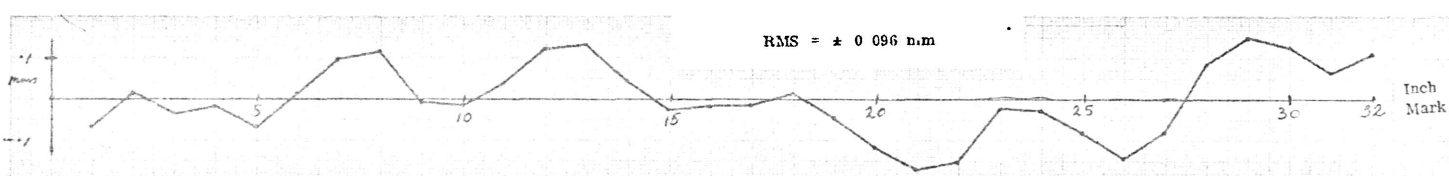

D. SUBTRACT 0.00755 cos $\frac{10\pi K}{28}$ from C.

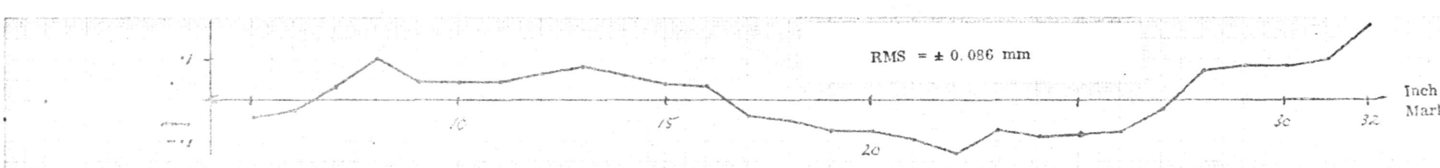

E. SUBTRACT 0.009 sin $\frac{2\pi K}{23}$ from D.

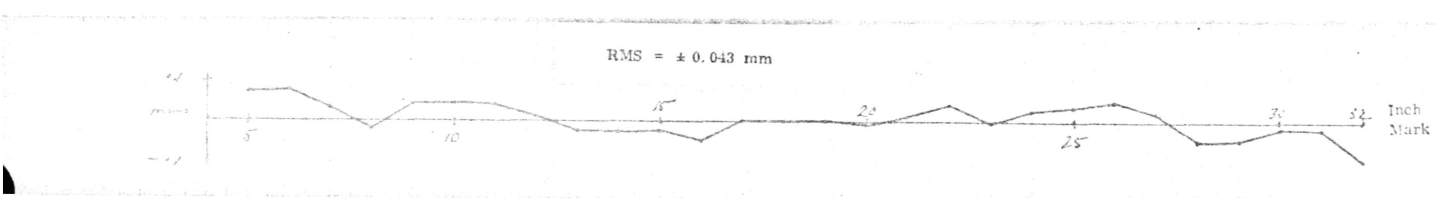

Figure 14 — Graph of Results

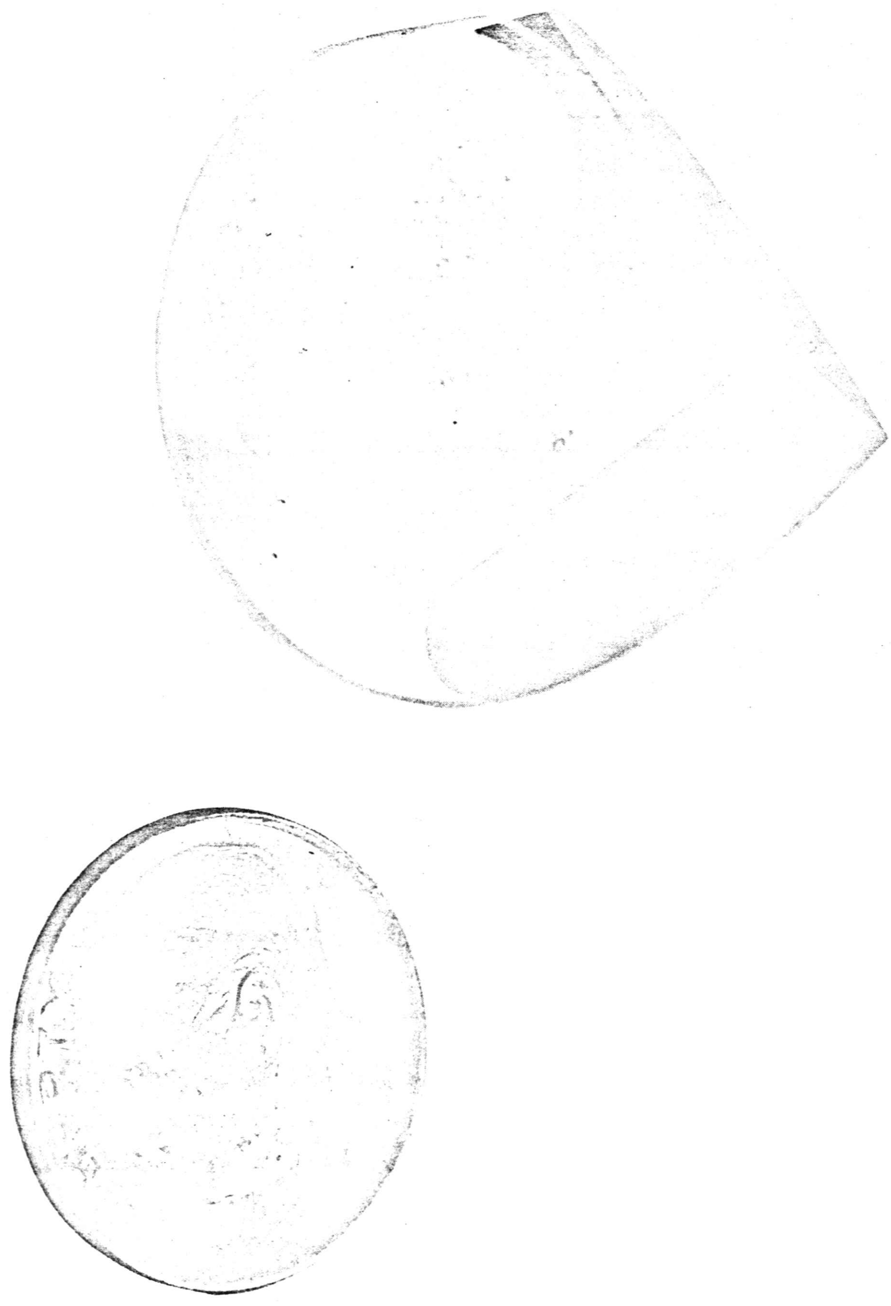

Figure 15 — Photograph of Corner Cube Reflector

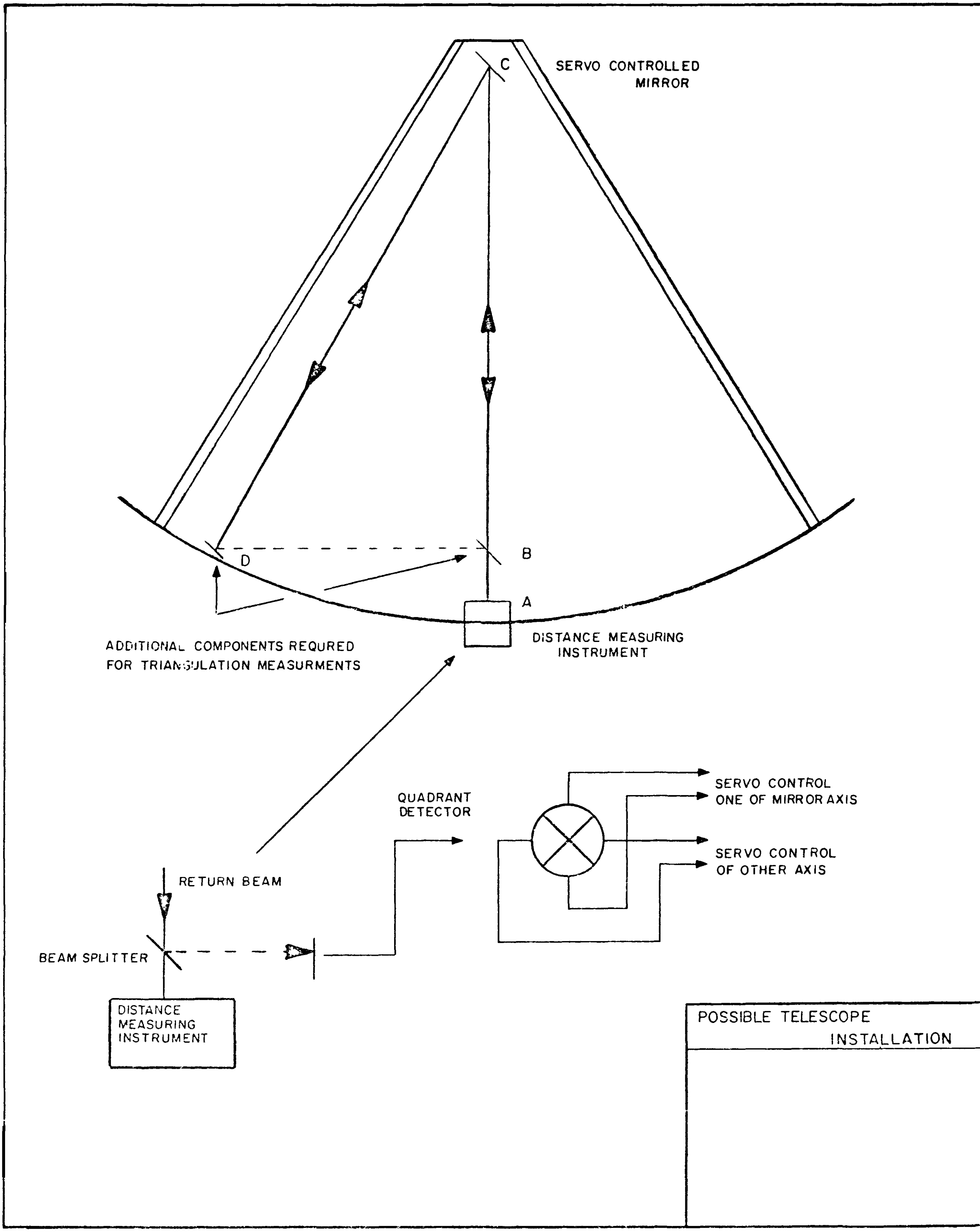

Figure 16 — Possible Telescope Installation

TABLE 1

Summary of Different Forms of Modulated Light Beam Instruments

Manufacturer and Model	Light Source	Modulating Frequency	Measurement Time	Accuracy	Readout	Phase Measurement Principle	Remarks
Plessey Model MA 100	Infrared light emitting diode.	75 MHz	3 secs	± 1 mm	Direct Digital Display	Mixed to 10 kHz and switched against internal reference path.	
Ziess SM-11	Infrared light emitting diode.	15 MHz	Approx. 20 secs	± 1 cm	Direct Digital Display	Mixed to IF and compared directly.	
Spectra-Physics Geodolite	Helium neon laser.	50 MHz	10 secs	± 1 mm	Direct Digital Display	Mixed to 4 kHz and compared directly.	Costs $50,000
Hewlett-Packard	Infrared diode.	25 MHz	Depends on operator.	± 2 mm	Mechanical.	Mixed to 25 kHz and compared with reference path. Nulled by operator.	
National Physics Laboratory England Mekometer III	Flash tube	492 MHz	Depends on operator.	± 0.1 mm	Mechanical.	Phases nulled optically by mechanically changing path length.	Not commercially available.
NRAO Described in this report.	Helium neon laser.	550 MHz	2.5 secs	± 0.07 mm	Direct Digital Readout	Mixed to 3.7 kHz and compared directly.	

TABLE 2

Test Over 60 m Path

Slope = −2.541099 ± 0.000145 cm

Intercept = 82.2613 ± 0.0027 cm

RMS (1σ) ± 0.00757 cm

Slope Corrected for Atmosphere = −2.541099 x 0.99964 = −2.540180 cm

Micrometer Position Inch	Digital Readout cm	Readout + $n\lambda$	Error cm
32	0.948	0.948	−0.002
31	3.492	3.492	−0.005
30	6.030	6.030	−0.002
29	8.564	8.564	+0.005
28	11.106	11.106	+0.005
27	13.651	13.651	+0.001
26	16.200	16.200	−0.007
25	18.735	18.735	−0.001
24	21.261	21.261	+0.014
23	23.809	23.809	+0.007
22	26.351	26.351	+0.006
21	1.594	28.901	−0.003
20	4.141	31.448	−0.009
19	6.671	33.978	+0.002
18	9.211	36.518	+0.004
17	11.756	39.063	0.000
16	14.305	41.612	−0.008
15	16.856	44.163	−0.018
14	19.388	46.695	−0.009
13	21.922	49.229	−0.002
12	24.452	51.759	+0.009
11	27.004	54.311	−0.002
10	2.236	56.849	+0.001
9	4.779	59.392	−0.001
8	7.314	61.927	+0.006
7	9.841	64.454	+0.020
6	12.398	67.011	+0.004
5	14.944	69.557	−0.001
4	17.497	72.110	−0.013
3	20.029	74.642	−0.004
2	22.563	77.176	+0.003
1	25.106	79.719	+0.001